

Fig. 3.1. Construction of a wave packet as a sum of harmonic waves ψ_n of different momenta and consequently of different wavelengths. Plotted are the real parts of the wave functions. The terms of different momenta and different amplitudes begin with the one of longest wavelength in the background. In the foreground is the wave packet resulting from the summation. (a) The situation for time $t = t_0$. All partial waves are marked by a circle at point $x = x_0$. (b) The same wave packet and its partial waves at time $t_1 > t_0$. The partial waves have moved different distances $\Delta x_n = v_n(t_1 - t_0)$ because of their different phase velocities v_n , as indicated by the circular marks which have kept their phase with respect to those in part a. Because of the different phase velocities, the wave packet has changed its form and width.

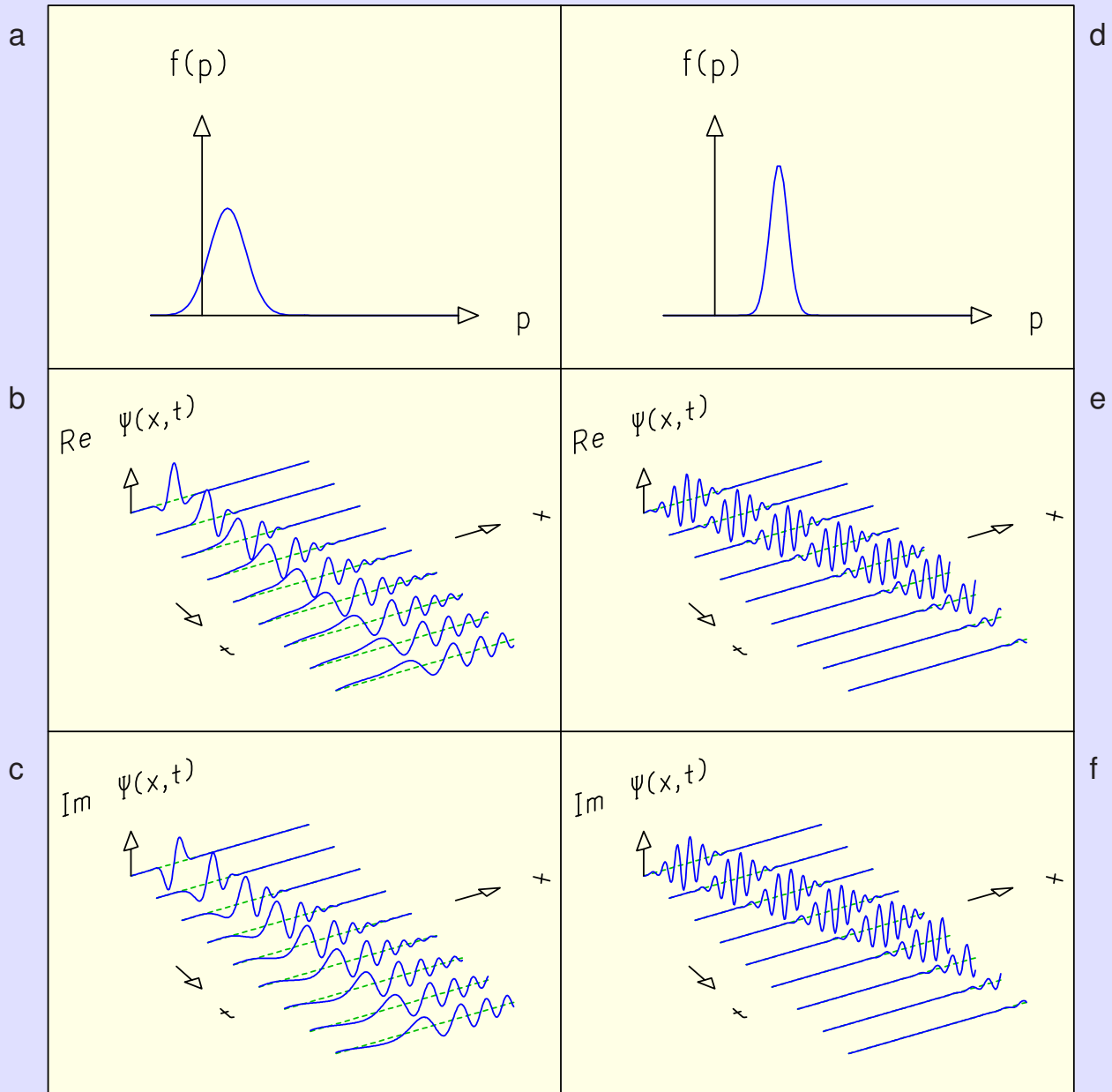


Fig. 3.2. (a, d) Spectral functions and time developments of (b, e) the real parts and (c, f) the imaginary parts of the wave functions for two different wave packets. The two packets have different group velocities and different widths and spread differently with time.

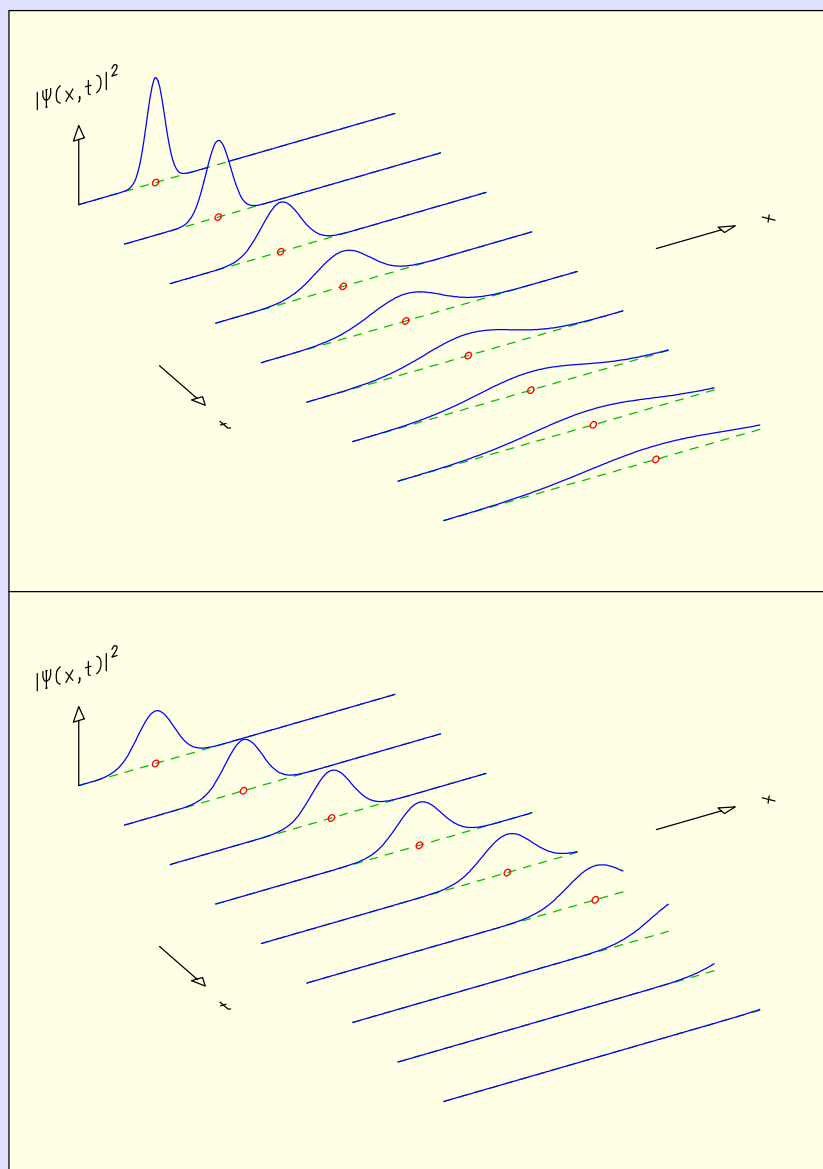


Fig. 3.3. Time developments of the probability densities for the two wave packets of Figure 3.2. The two packets have different group velocities and different widths. Also shown, by the small circles, is the position of a classical particle moving with a velocity equal to the group velocity of the packet.

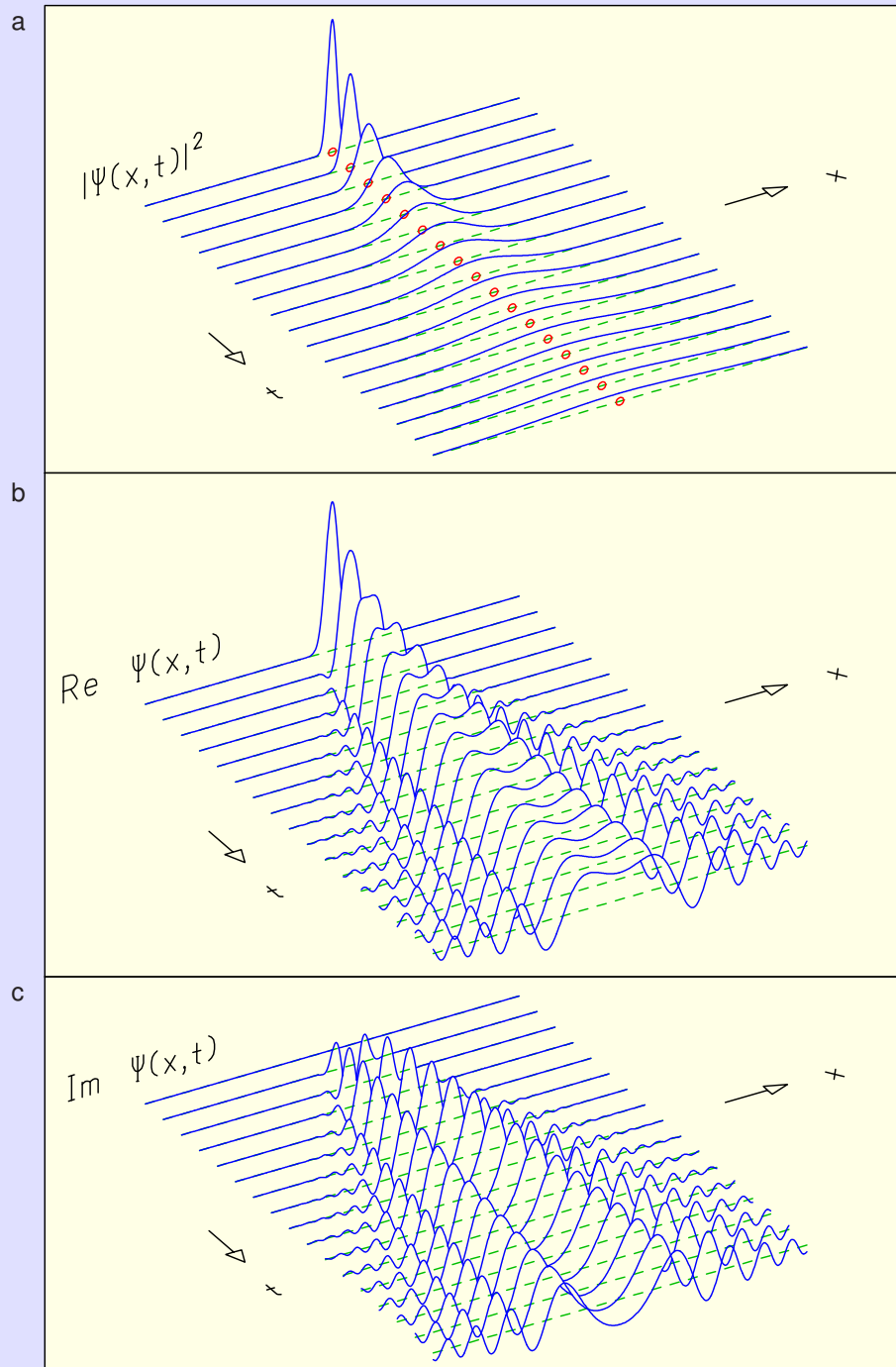


Fig. 3.4. Time developments of the probability density for a wave packet at rest and of the real part and the imaginary part of its wave function.

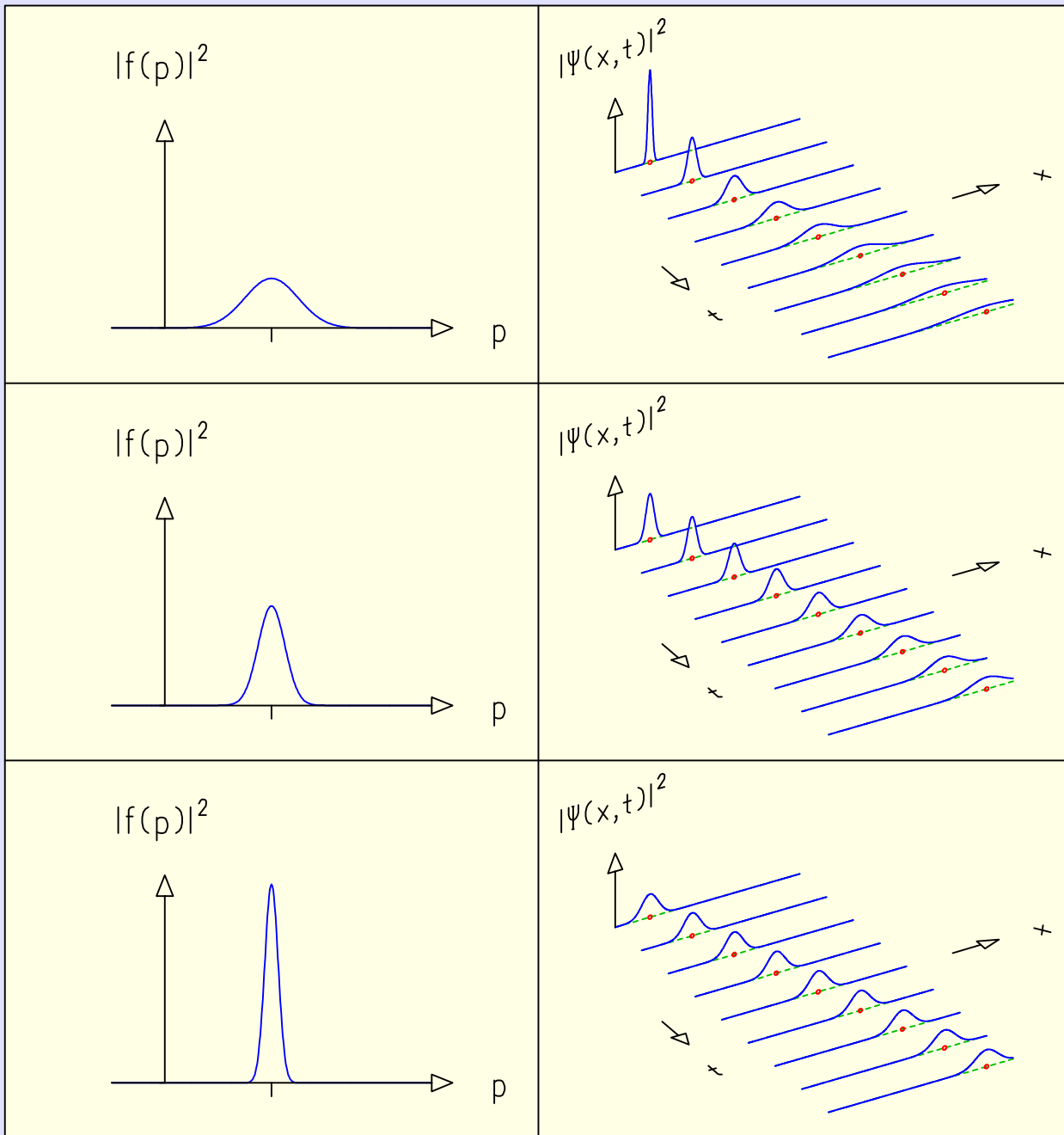


Fig. 3.5. Heisenberg's uncertainty principle. For three different Gaussian wave packets the square $f^2(p)$ of the spectral function is shown on the left, the time development of the probability density in space on the right. All three packets have the same group velocity but different widths σ_p in momentum. At $t = 0$ the widths σ_x in space and σ_p in momentum fulfill the equality $\sigma_x \sigma_p = \hbar/2$. For later moments in time the wave packets spread in space so that $\sigma_x \sigma_p > \hbar/2$.

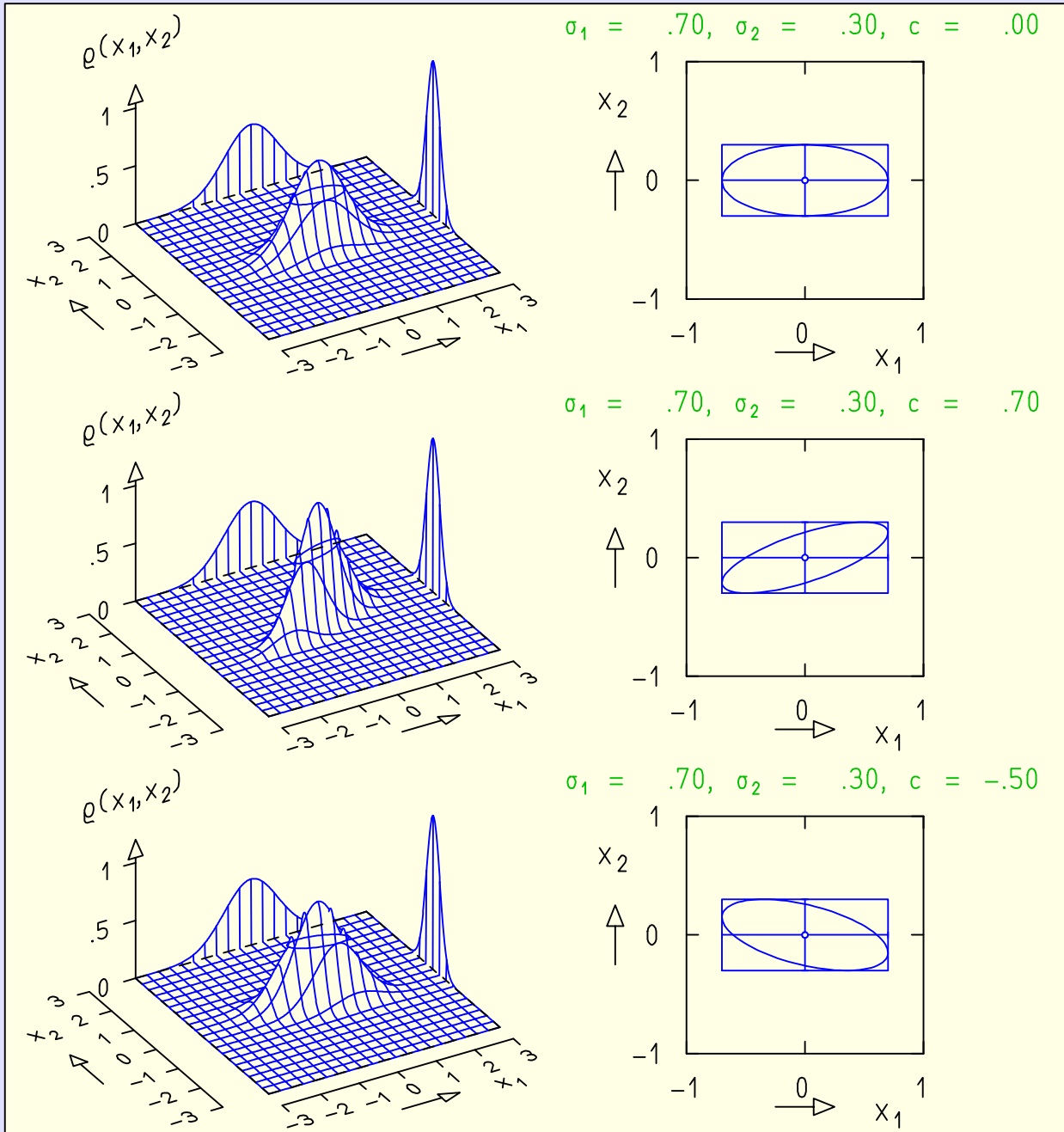


Fig. 3.6. Bivariate Gaussian probability density $\rho(x_1, x_2)$ drawn as a surface over the x_1, x_2 plane and marginal distributions $\rho_1(x_1)$ and $\rho_2(x_2)$. The latter are drawn as curves over the margins parallel to the x_1 axis and the x_2 axis, respectively. Also shown is the covariance ellipse corresponding to the distribution. The rectangle circumscribing the ellipse has the sides $2\sigma_1$ and $2\sigma_2$, respectively. The pairs of plots in the three rows of the figure differ only by the correlation coefficient c .

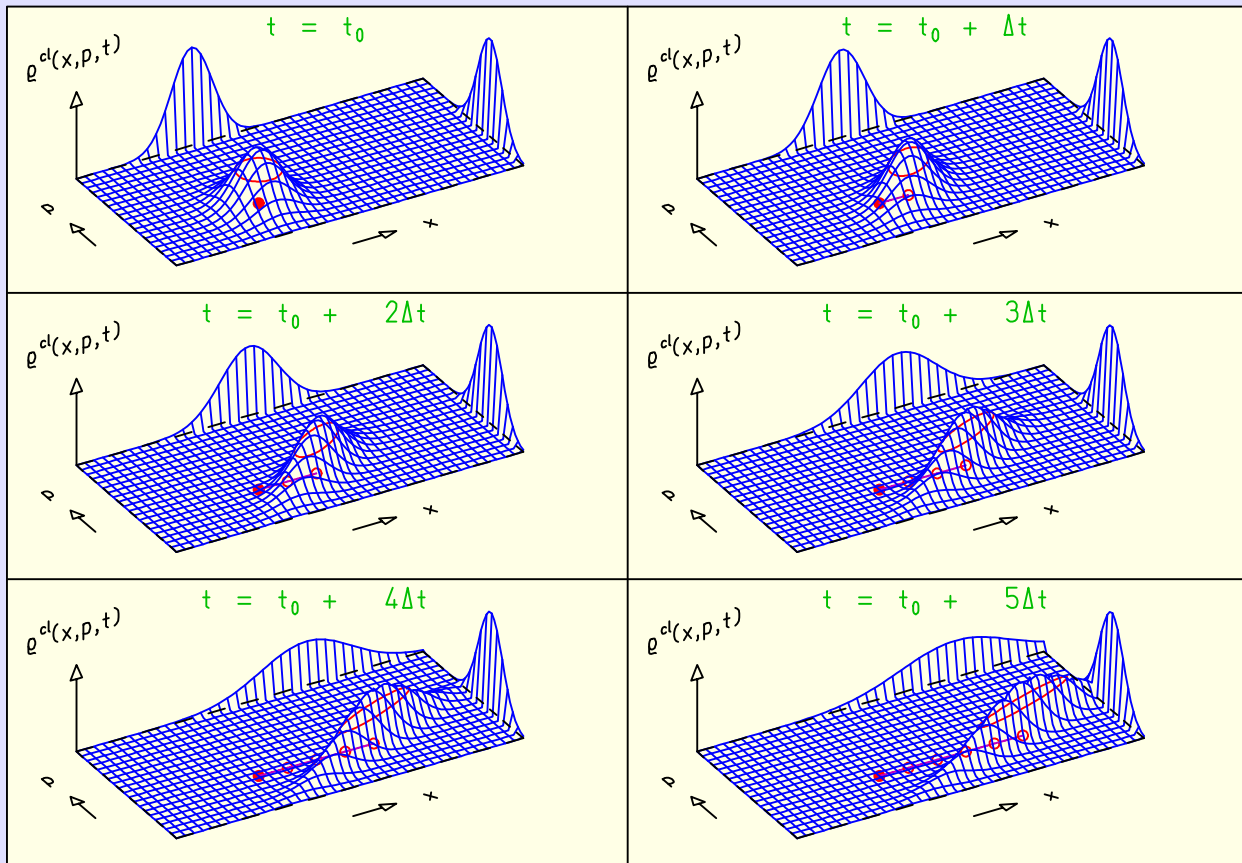


Fig. 3.7. Time development of the classical phase-space probability density $\rho^{\text{cl}}(x, p, t)$ for a free particle with uncertainty in position and momentum. Also shown are the marginal distributions $\rho_x^{\text{cl}}(x, t)$ in the back and $\rho_p^{\text{cl}}(p, t)$ on the right-hand side of the plots.

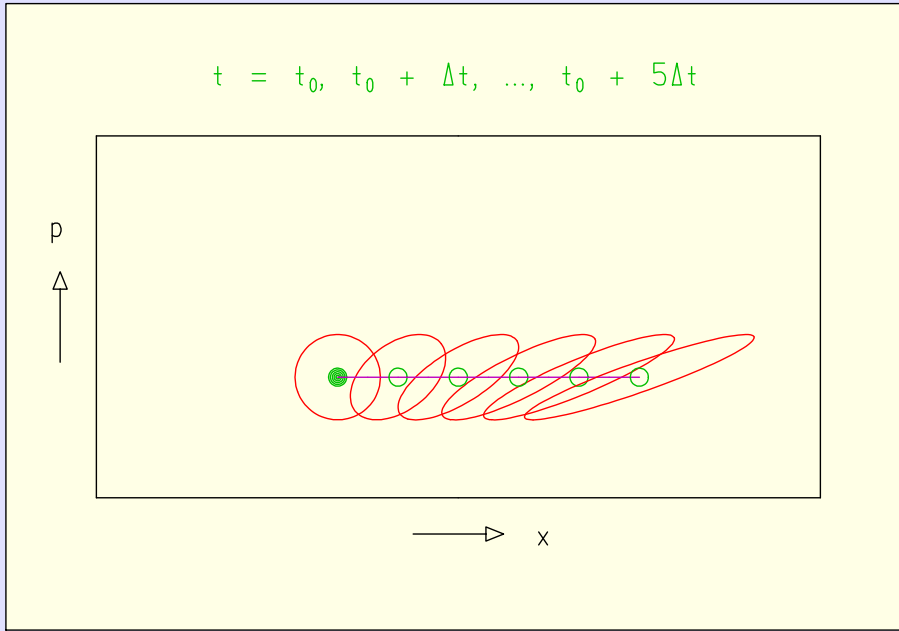


Fig. 3.8. Motion of the covariance ellipse in phase space which characterizes the classical space probability density $\rho^{\text{cl}}(x, p, t)$ of a free particle. The ellipse is shown for six moments of time corresponding to the six plots in Figure 3.7. The center of the ellipse (indicated by a small circle) moves with constant velocity on a straight trajectory. The rectangle circumscribing the covariance ellipse has sides of lengths $2\sigma_x(t)$ and $2\sigma_p(t)$, respectively. While σ_p stays constant, σ_x increases with time. For $t = t_0 = 0$ there is no correlation between position and momentum (ellipse on the far left) but with increasing time a strong positive correlation develops.